Powder Technology 408 (2022) 117777

Contents lists available at ScienceDirect

Powder Technology

journal homepage: www.journals.elsevier.com/powder-technology

On the comprehension of the gas split in loop seal devices

M. Suárez-Almeida *, A. Gómez-Barea

Chemical and Environmental Engineering Department, Escuela Técnica Superior de Ingeniería, University of Seville, Camino de los Descubrimientos s/n, 41092 Seville, Spain

HIGHLIGHTS

- Gas splitting into the chambers of a loop seal is a key issue difficult to predict.
- The gas distribution was experimentally assessed in an isolated loop seal.
- Loop seal operation as non-mechanical valves leads to non-ideal gas-solids flows.
- Non-ideal gas-solids flow pattern establishes the gas splitting into the chambers.
- The study gives insights on how to control the solids circulation with a loop seal.

GRAPHICAL ABSTRACT

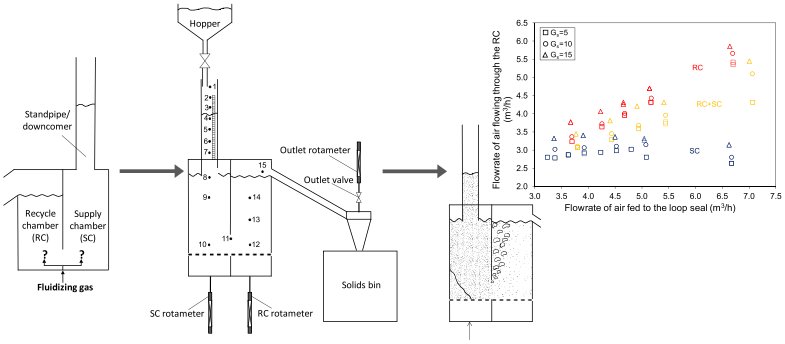

ARTICLE INFO

Keywords:
Loop seal
Solids circulation
Supply chamber
Recycle chamber
Standpipe
Fluid dynamics

ABSTRACT

Gas distribution through the chambers of a loop seal in circulating fluidized bed (CFB) units is still difficult to predict and often misunderstood. Dedicated experiments were carried out in an isolated loop seal to assess how the gas fed into a loop seal is distributed under different aeration modes (through the recycle chamber, the supply chamber and both chambers), aeration flowrates and solids fluxes. Experimental results shed light on the non-ideality of the gas-solids flows occurring in these units and, in combination with theoretical considerations, it is demonstrated why semi-empirical models cannot effectively describe the performance of loop seals operating as non-mechanical valves. Recommendations are given for the optimization of the operation of a loop seal as a non-mechanical valve in a solids circulating loop. A method is proposed to characterize the performance of a loop seal in a CFB unit from measurements of that loop seal in isolation mode.

1. Introduction

Non-mechanical valves constitute a superior choice for solids circulating and gas sealing in CFB units operated with Geldart B particles, due to the absence of moving parts, low cost and operational simplicity [1,2]. Compared to L-valves and J-valves, loop seals present several advantages: safer operation due to the isolation of the standpipe from the pressure fluctuations in the riser, operational capability both as non-mechanical valve and as a solids circulation device, and more flexible design to allocate devices like heat exchangers in CFB units such as boilers. Although loop seals have been successfully used in industrial processes (mainly in CFB boilers and catalytic reactors), there is still a lack of knowledge to enable the design and operation on a fundamental basis. One controversial point is whether a loop-seal performs merely as

* Corresponding author.
E-mail address: msalmeida@us.es (M. Suárez-Almeida).

https://doi.org/10.1016/j.powtec.2022.117777
Received 3 May 2022; Received in revised form 11 July 2022; Accepted 22 July 2022
Available online 29 July 2022

an automatic solids flow device or as a non-mechanical valve with the capability of regulating the solids flux in a CFB loop. While most authors recognize the capacity of the loop seal for controlling solids circulation under some conditions [3–7], some argue that the solids flux is merely governed by the riser aeration [8]. The design and operating conditions of the loop seal determine which of these statements apply for a given CFB unit. In large CFB boilers, where the loop seal is rather small compared to the combustor chamber (riser), the solids flux is usually controlled by the fluid dynamics of the riser. However, the operation of the loop seal as a non-mechanical valve could be crucial in emerging fluidized beds like those dealing with technologies such as chemical-looping combustion and reforming, thermochemical energy storage based on gas-solids reversible reactions, or the production of renewable energy in hybrid processes like steam gasification of biomass in dual fluidized bed gasifiers using solar energy [9–11]. These technologies require solids circulating and gas sealing but also high flexibility of solids circulation to adapt the operation to different scenarios.

Designing and optimizing loop seals for fluidized bed applications in the near future requires a robust and comprehensive knowledge of the fluid dynamics of these units. Some attempts have been made, both under modeling and experimental work, to assess the performance of the loop seal, but clear and general conclusions are still lacking. As a result, loop seal systems are still empirically designed, often ignoring fundamental considerations, thereby hindering optimization of these devices.

This paper intends to clarify existing knowledge of the fluid dynamics of loop seals on the basis of conclusions obtained from experimental work conducted in an isolated loop seal cold flow model. Dedicated experiments were carried out to assess, through direct measurements, the gas split through the chambers of the loop seal as a function of the gas flowrate, the location of the aeration points and the solids flux. The experimental results, together with their implications for the design and operation of loop seals within solids circulating systems, are discussed and compared with the existing literature. In addition, the way in which results from an isolated loop seal should be used to predict the performance of and to design a loop seal coupled to a CFB unit is presented.

2. Theory

Gas distribution along the loop seal (Fig. 1) is the key parameter determining the performance of the system, i.e. the flow state of the supply chamber (SC)/standpipe/downcomer (usually regarded as a dense bed in minimum fluidization or a moving bed) and the regulation capability of the solids circulation. This issue has been a matter of concern over the years when trying to model and predict the performance of loop seals. A summary is given below to bring to light the interpretations and assumptions made by different authors that often contradict each other.

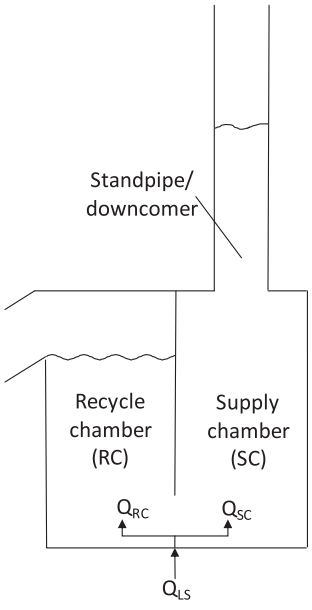

Fig. 1. Sketch of the main parts of a loop seal together with the distribution of the total fed gas (Q_{LS}) between the two chambers.

2.1. Gas distribution and aeration mode

Gas distribution along the loop seal has traditionally been assessed based on estimations from standpipe pressure and height measurements (assumed to be in a defluidized state) [12–15] and through the use of gas tracers [7,16–20], but the gas flowrate has never been directly measured until now. Most authors agree that the majority of the air fed to the loop seal leaves the unit through the RC (provided the SC is not fluidized) [3,7,14,21]. It has been experimentally demonstrated that increasing the solids circulation leads to a higher resistance for gas to flow up through the standpipe. For a given loop seal aeration, there is a threshold in the solids velocity, at which gas is dragged by solids in the standpipe [13,14,16], resulting in a higher flowrate of gas through the RC than that fed through the loop seal. Moreover, when the solids circulation increases as a result of an increase in the loop seal aeration, there is a critical aeration flowrate at which the downward gas flow through the standpipe is maximum (or the upward gas is minimum if the loop seal is operated under no dragging). Beyond this critical aeration, the downward gas flowrate rapidly decreases, the flow direction reverses upward and the standpipe becomes fluidized [15,17].

The aeration mode has a significant effect on gas distribution along the loop seal (i.e., on its performance) and has been the subject of many studies. Although many combinations have been analyzed, the performance of the loop seal when aerated under the simplest mono-chamber modes, i.e., separately through the SC and through the RC, has received less attention. The effect of mono-chamber aeration on the solids circulation was firstly assessed in [22] leading to unclear differences between the aeration modes and, later, in [23], where it was concluded that aerating through the SC is more effective for controlling the solids circulation, since it results in a higher solids flux for a given aeration flowrate. A more dedicated study was carried out in [24] where the SC aeration resulted in the highest solids circulation, while the RC resulted in a wider range of control of the solids circulation. Although these works demonstrate that a loop seal can operate under any mono-chamber aeration, conclusions on the operation of the loop seal under its simplest aeration modes are still unclear. The experiments carried out in this work (detailed in Section 3.2) intend to fill this gap.

The reason behind the higher efficiency of the aeration through the SC in the control of solids circulation rests on the gas distribution and its effect on the loop seal performance as a non-mechanical valve. The operation of the loop seal as a non-mechanical valve takes place when the standpipe is under moving bed regime (also referred to as a transitional packed bed) and the pressure drop per unit length is controlled by drag forces between gas and solid particles. This pressure drop is regulated by the gas-solids relative velocity (estimated, for instance, through an expression such as that proposed by Ergun, Eq. (5)). Under this operation mode, a change in the gas-solids relative velocity results in a change in the pressure gradient along the standpipe, which needs to reallocate the solids to keep the pressure balance around the CFB loop, leading to a change in the solids circulation. Therefore, the range of solids circulation control of a non-mechanical valve is determined by the ability to change the gas-solids relative velocity before it reaches the minimum fluidization velocity (related to the flow of solids). Feeding the air through the SC leads to an increased amount of gas flowing through the standpipe (compared to the same air fed through the RC) and therefore, to a higher pressure drop in the standpipe and solids circulation. More details on the operation of the loop seal in a CFB loop and

on the gas split under different aeration modes are given in Section 4.2.1 and Section 4.1.3, respectively.

The principle of the operation of loop seals has been a matter of discussion over the years, resulting in a wide variety of studies with different approaches. Traditionally, aeration through the RC was considered essential, while that of the SC simply constituted an optional way of aiding the solids flow down the standpipe and ensure smooth operation [21,25,26]. Moreover, some authors still wrongly state that to operate the standpipe in a non-fluidized mode, the aeration through the SC should not exceed that of minimum fluidization [27,28]. In addition to the previously mentioned works, the superior performance of the SC aeration for controlling the solids circulation is also recognized by [3,5,19], but only in [19] is the possibility of operating under SC mono-chamber aeration recognized. Although operational limitations, such as the appearance of slugging reported in [25] for a DFB gasifier, tend to tarnish the advantages of aerating through the SC, new designs have already been proposed to stabilize the operation [29]. Vertical aeration through the SC/standpipe has been extensively studied as a way to optimize the performance of the loop seal as a non-mechanical valve [29–31], promoting the gas flowing through the standpipe and avoiding the gas bypassing through the opening. Other works have assessed different aerations combining both bottom and side aerations [32,33], although the results are not comprehensive enough for generalization. An extensive analysis of the operation of the loop seal in a DFB unit is carried out in [7], where different aeration modes are analyzed and the superior performance of aerating through the SC is also demonstrated for these units (in which the gas distribution along the loop seal plays an important role since the leakage between reactors needs to be avoided [7,20]).

2.2. Modeling barriers

Loop seals may be considered the heart of a CFB plant. As a result, models appear to be excellent tools, not only to understand the performance of the loop seal, but also to optimize its operation within the solids circulating loop. Many modeling attempts have been made over the years, but certain features of these units have prevented them from achieving success. This section presents the barriers found when modeling the fluid dynamics of a loop seal and reviews different works dealing with loop seals modeling.

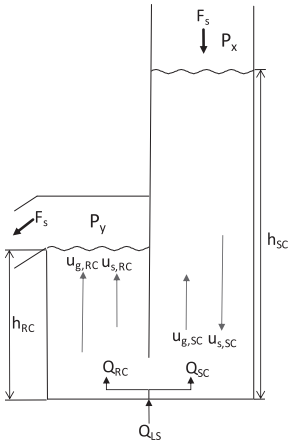

Fig. 2. Solids and gas velocities and fed gas distribution in the two chambers of a loop seal. The downcomer is considered an extension of the SC in this sketch; F_s represents the flowrate of solids and P_x and P_y the pressure at the inlet and outlet of the SC and RC, respectively, being $P_y > P_x$.

$$\varepsilon_{RC} = \delta + (1-\delta)\varepsilon_{mf} \tag{3}$$

A bubble fraction equal to zero represents the operation of the RC under incipient fluidization. The expansion of the bed can be calculated with a model estimating the expansion behavior in bubbling beds such as that in [34],

$$\delta = \frac{1}{1 + \frac{1.3\left(0.15+\left(u_{g,RC}-u_{s,RC}\right)\varepsilon_{RC}-u_{mf}\right)^{1/3}}{0.26+0.7e^{-3300\ d_p}}\left(\left(u_{g,RC}-u_{s,RC}\right)\varepsilon_{RC}-u_{mf}\right)^{-0.8}} \tag{4}$$

Assuming that the gas-solids relative velocity in the SC is that allowing the operation under moving bed regime, the pressure drop is given by the modified Ergun equation [35], where the bed voidage can be regarded, as a first approach, constant and equal to that at minimum fluidization.

$$\varepsilon_{SC} = \varepsilon_{mf} \tag{6}$$

$$\Delta P_{SC} = \left(150\frac{(1-\varepsilon_{SC})^2}{{\varepsilon_{SC}}^2}\frac{\mu_g}{\phi\,{d_p}^2}\left(u_{g,\mathrm{SC}}+u_{s,\mathrm{SC}}\right) + 1.75\frac{(1-\varepsilon_{SC})}{\varepsilon_{SC}}\frac{\rho_g}{\phi\,d_p}\left(u_{g,SC}+u_{s,\mathrm{SC}}\right)^2\right)h_{SC} \tag{5}$$

The fluid dynamics of an isolated loop seal, such as that presented in Fig. 2, can be studied by a simple model based on the pressure balance along the unit. The unit in Fig. 2 is fed by a constant flow of solids (F_s) and a gas flowrate (Q_{LS}), while the solids inventory is adapted by the height of solids in the SC (h_{SC}) and, to a lesser extent, by the bed expansion in the RC, to balance the pressure along the loop seal. Assuming that the pressure drop along the opening is small compared to that of the chambers, it follows,

$$\Delta P_{SC} = \Delta P_{RC} + \Delta P_{yx} \tag{1}$$

The RC always needs to be fluidized to allow the solids circulation thus, the pressure drop is given by the hydrostatic pressure of the head of solids along the RC up to the weir (h_{RC}),

$$\Delta P_{RC} = \rho_p(1-\varepsilon_{RC})h_{RC}\,g \tag{2}$$

The bed voidage (ε_{RC}) can be estimated considering the bubble fraction (δ) as,

When the superficial gas-solids relative velocity in the SC, $(u_{g,SC}+u_{s,SC})\varepsilon_{SC}$, is higher than the minimum fluidization velocity, the SC operates under fluidized flow. In this case, the modeling approach followed for the RC Eqs. (2)–(4) can be applied to the SC, but taking into consideration the gas-solids relative velocity in the SC and the height of solids in the SC. However, this operation is rarely applied to loop seals operating in actual circulating loops since, apart from entailing higher costs regarding the increased need for fluidizing agent, operating the SC under vigorous bubbling can lead to instabilities in the operation, affecting the efficiency of the cyclone in CFB units and leading to contamination/dilution of the reacting system in DFB units.

The actual solids and gas velocities in both chambers are defined as,

$$u_{s,RC} = \frac{F_s}{\rho_p(1-\varepsilon_{RC})A_{RC}} \tag{7}$$

$$u_{s,SC} = \frac{F_s}{\rho_p(1-\varepsilon_{SC})A_{SC}} \tag{8}$$

$$u_{g,RC} = \frac{u_{0,RC}}{\varepsilon_{RC}} \tag{9}$$

$$u_{g,SC} = \frac{u_{0,SC}}{\varepsilon_{SC}} \tag{10}$$

where the superficial gas velocities are given by considering the gas flowing through each chamber, the sum of them being equal to the introduced gas through the loop seal, Q_{LS},

$$u_{0,RC} = \frac{Q_{RC}}{A_{RC}} \tag{11}$$

$$u_{0,SC} = \frac{Q_{SC}}{A_{SC}} \tag{12}$$

$$Q_{LS} = Q_{SC} + Q_{RC} \tag{13}$$

To sum up, this simple model accounts for 13 equations and 14 unknowns (ΔP_{RC}, ΔP_{SC}, ε_{RC}, ε_{SC}, δ, $u_{g,RC}$, $u_{g,SC}$, $u_{s,RC}$, $u_{s,SC}$, $u_{0,RC}$, $u_{0,SC}$, h_{SC}, Q_{RC} and Q_{SC}), the rest of the parameters constituting known data. Obviously, the same balance results from considering the SC under fluidized flow. Therefore, it can be concluded that an additional relation is necessary to solve the model, predicting the gas split through the chambers of a loop seal.

Gas distribution through the loop seal is determined by the resistance to gas-solids flow offered by the SC, the horizontal passage (opening) and the RC. A proper model of these resistances by a momentum balance, considering both gas and solid phases, provides the required closure relation. Under certain operating conditions, there is a limiting resistance, enabling the simplified treatment of the loop seal model. However, the operating conditions and geometry of loop seals found in the literature greatly vary from each other, making a comprehensive generalization of loop seal performance difficult. For these reasons, none of the models developed to date are general enough to predict the performance of loop seals.

There are only two published models that, although unsuccessful, theoretically provide a relation that could be used to close the model above [36,37]. Both approaches set in the RC the closure relation, considering the RC as that which is limiting the flow of solids and therefore, setting the gas distribution. However, the RC is always under fluidized flow, so it never limits the flow of solids and both approaches fail on a fundamental basis.

In [36] the sharp-crested weir theory was applied to the solids overflow from a loop seal leading to an empirical relation. However, it is not clear from publications [1,36] if the solids flow rate is related to the height of the expanded bed above the weir or to the height of the weir. Only the latter option would enable to close the model since the expanded bed above the weir is unknown. For a given solids flux, the relation allows for calculation of the voidage in the RC (since the voidage in the bed above the weir is assumed to be equal to that in the RC), thereby establishing the gas distribution. This theory has received neither more attention nor experimental validation over the years.

In the model developed in [37] the required closure relation is provided by a global force balance in the recycle chamber. However, it can be verified by the equations of the model that the gas-solids relative velocity in the RC, the voidage at the RC and, therefore, the pressure drop along the RC, are independent of the operating conditions, so the model is not able to capture the measure trends. This model intended to describe the operation of a loop seal aerated only through the RC with the standpipe operating under moving bed regime. Later, a similar approach was extended to assess the operation of a loop seal aerated by both the RC and the SC in which both chambers were assumed to be fluidized [38]. Although both models are contestable, they represent the only attempts at comprehensively describing the fluid dynamics of a loop seal considering differences in the operation due to the aeration mode.

In [39] a momentum balance in the SC is used as the closure relation to determine the gas division through a standpipe joined to a fluidized bed. This approach is applicable to narrow standpipes (where the solids-wall friction may be significant) connected in series to a fluidized bed, but it is rarely valid in loop seal non-mechanical valves in circulating devices (with wider standpipes connected to the RC by a horizontal passage which offers significant resistance to gas-solids flow). In most models the resistance through the horizontal passage (opening) is either neglected [10,37,38,40] or considered as that between two joined fluidized beds [41]. No published work has considered the resistance through the opening as that limiting the flow for setting the gas split in loop seal units.

Other modeling studies have applied assumptions for the gas distribution or semi-empirical correlations. The first attempts at modeling dealt with validating experimental measurements from an isolated loop seal [21] and analyzing the performance of a loop seal in a CFB loop [42]. Both assumed a constant fraction of gas flow through the RC equal to 9.5% as correlation of experimental measurements in [21]. In [43] the performance of the loop seal was assessed (to describe the fluid dynamics of a CBF unit) using an empirical correlation of the pressure drop with the solids flux, particle properties and loop seal diameter. This approach may fit measurements of a particular unit, but it does not provide a comprehensive understanding of the performance of a loop seal on a fundamental basis.

A model based on the pressure drop of the defluidized supply chamber and the horizontal channel was developed in [44] to estimate the pressure at the bottom of the recycle chamber of an isolated loop seal. Based on the same unit, a model was developed in [40] to estimate the concentration of solids in the RC and the height of solids in the SC based on a force balance in the RC. In both models the gas distribution was arbitrarily set, not being subjected to any fundamental or empirical consideration.

The model proposed in [45] is based on a function tending to a constant value as the aeration is increased, whose parameters are obtained through correlation of experimental data. Once the parameters are found, the model is able to predict the solids circulation in a loop seal as a function of the fluidization number (ratio between the actual and minimum fluidization velocity). Although the authors attempted to provide the model a fundamental background, it is far from describing the performance of a loop seal from a fundamental point of view.

A general law to model loop seals has yet to be proposed. None of the models developed to date are general enough to predict the performance of loop seals. Those based on correlations are only applicable to the units from which the correlated measurements were obtained, while those based on theoretical approaches have failed in their attempts since they have not been able to ascertain the limiting factors leading to the gas split between the chambers (key aspects, such as the aeration mode, have been overlooked). The experimental work presented here clearly demonstrates that theoretical prediction of the operation of a loop seal requires a more careful modeling effort than those offered by the models developed to date.

3. Experimental

3.1. Experimental setup

An experimental cold flow model was used to study the fluid dynamics of a loop-seal. The system was isolated from an existing CFB to dedicatedly study the gas and solid motions in the different parts of the loop seal. The rig, presented in Fig. 3, consists of a hopper joined to a solids discharge system (pipe and valve for controlling the solids flux) and a loop seal joined to a cyclone which collects the circulating solids leaving the system into a bin. Two rotameters are used to control the gas flowrate separately, one to feed the gas to the supply chamber (SC) and another one to the recycle chamber (RC) (the wind boxes of the SC and RC are completely separated from each other). The gas leaving the

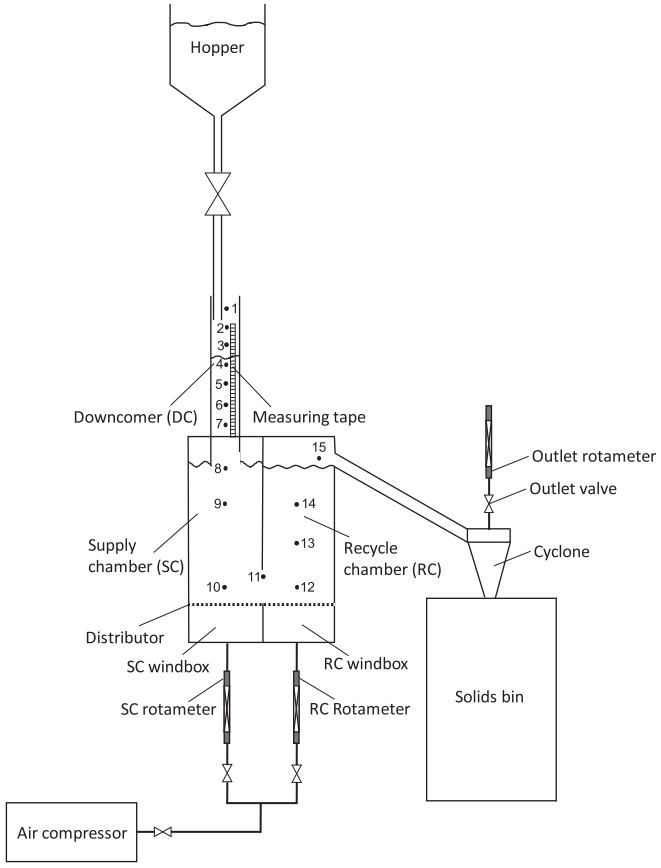

Fig. 3. Experimental rig (numbered dots represent the pressure taps; dot number 1 is never covered by solids so it measures the atmospheric pressure).

cyclone, i.e., that passing through the RC, is measured using another rotameter, which requires a valve at the inlet to stabilize the float. A measuring tape is set along the downcomer to measure the height of solids during the tests. Fifteen pressure taps are allocated along the loop seal. A data logger and a computer are used to continuously (every second) register the pressure measurements.

The downcomer has a 0.093 m internal diameter, SC and RC have a cross section of 0.119 × 0.130 m^2 while the section of the opening is 0.130 × 0.055 m^2. The height of the SC above the distributor is 0.270 m and that of the RC until the discharging pipe is 0.155 m. The measuring tape is located just above the SC but the downcomer is 0.060 m below this point (0.02 m along the junctions and 0.04 m inside the SC). The gas distributor is a 4 mm thick perforated plate with 45 holes of 2 mm diameter in each chamber and a fine metallic grid to avoid the falling of solids back to the plenum. The pressure drop through the distributor was below 15 mbar for all the tests.

The bed material was glass beads with a particle size of 150–250 μm, a density of 2503 kg/m^3 (Geldart B) and an experimental minimum fluidization velocity at room temperature of 0.04 m s^{-1}. Air at room temperature was used as fluidizing agent.

3.2. Experiments

During the tests the solids flux was kept constant while varying the gas flowrate fed to the system, as well as the aeration mode. Solids fluxes of 5, 10 and 15 kg m^{-2} s^{-1} (referring to the SC cross section) were tested at three different aeration modes (only RC, only SC and both chambers). The same gas flowrate was introduced through each chamber in experiments aerated under both chambers. For each test the pressure at taps presented in Fig. 3 was continuously measured and registered for two minutes of operation after reaching the steady state. The latter was considered to be attained when the height of solids in the downcomer reached a constant value on the measuring tape. The gas distribution along SC and RC was calculated by the difference between the introduced air and that leaving the system through the RC.

Two sets of tests were carried out: one with the outlet rotameter (and the outlet valve) to measure the gas leaving the RC and, another, removing both the outlet rotameter and valve, to assess the effect of this outlet constriction on the gas and solids distribution along the loop seal. In those tests carried out with the outlet rotameter, the outlet valve was always kept in the same position. A minimum of 2 tests were conducted for each of the operating conditions to guarantee repeatability. The tests carried out (145 in total, 108 with the outlet valve and 37 without outlet valve) are summarized in Table 1.

Table 1
Summary of tests (fed gas velocity referred to the cross section of a single chamber; G_s referred to the cross section of the SC).

Aeration mode	Air flowrate (m^3 h^{-1})	Fed gas velocity (m s^{-1})	Number of tests		
			G_s = 5 kg m^{-2} s^{-1}	G_s = 10 kg m^{-2} s^{-1}	G_s = 15 kg m^{-2} s^{-1}
			Tests with outlet rotameter		
SC	3.3	0.059	2	–	–
	3.5	0.063	2	2	2
	3.7	0.066	3	–	–
	4.0	0.072	2	2	2
	4.3	0.077	2	–	–
	4.6	0.083	2	2	2
	4.9	0.088	2	–	–
	5.2	0.093	2	2	2
	6.8	0.122	3	2	2
SC + RC	3.9	0.070	3	2	2
	4.5	0.081	2	2	2
	5.0	0.090	2	2	2
	5.5	0.099	2	2	2
	7.2	0.129	2	2	2
RC	3.8	0.068	2	2	3
	4.3	0.077	2	2	2
	4.8	0.086	3	2	4
	5.3	0.095	3	2	4
	6.8	0.122	2	2	2
			Tests without outlet rotameter		
SC	3.3	0.059	3	–	4
	3.8	0.068	2	–	2
	5.0	0.090	2	–	4
	6.5	0.117	2	–	2
RC	3.6	0.065	2	–	2
	4.2	0.075	2	–	2
	5.0	0.090	2	–	2
	6.5	0.117	2	–	2

4. Results and discussion

Experiments were carried out for constant solids fluxes varying the aeration flowrate. For a given solids flux, after a change in the air flowrate fed, the solids inventory in the system varied, adapting the pressure throughout the unit to allow the operation under the new conditions. This operation provides insights into the behavior of an isolated loop seal, but the knowledge gained can be used to describe the performance of the loop seal connected to a CFB unit where (most of the time) the solids inventory is kept constant while the solids flux is the variable to be controlled. Experimental results obtained in the isolated loop seal under constant solids fluxes are presented in Section 4.1, while discussion on how this information is used in a loop seal coupled to a CFB unit is discussed in Section 4.2.

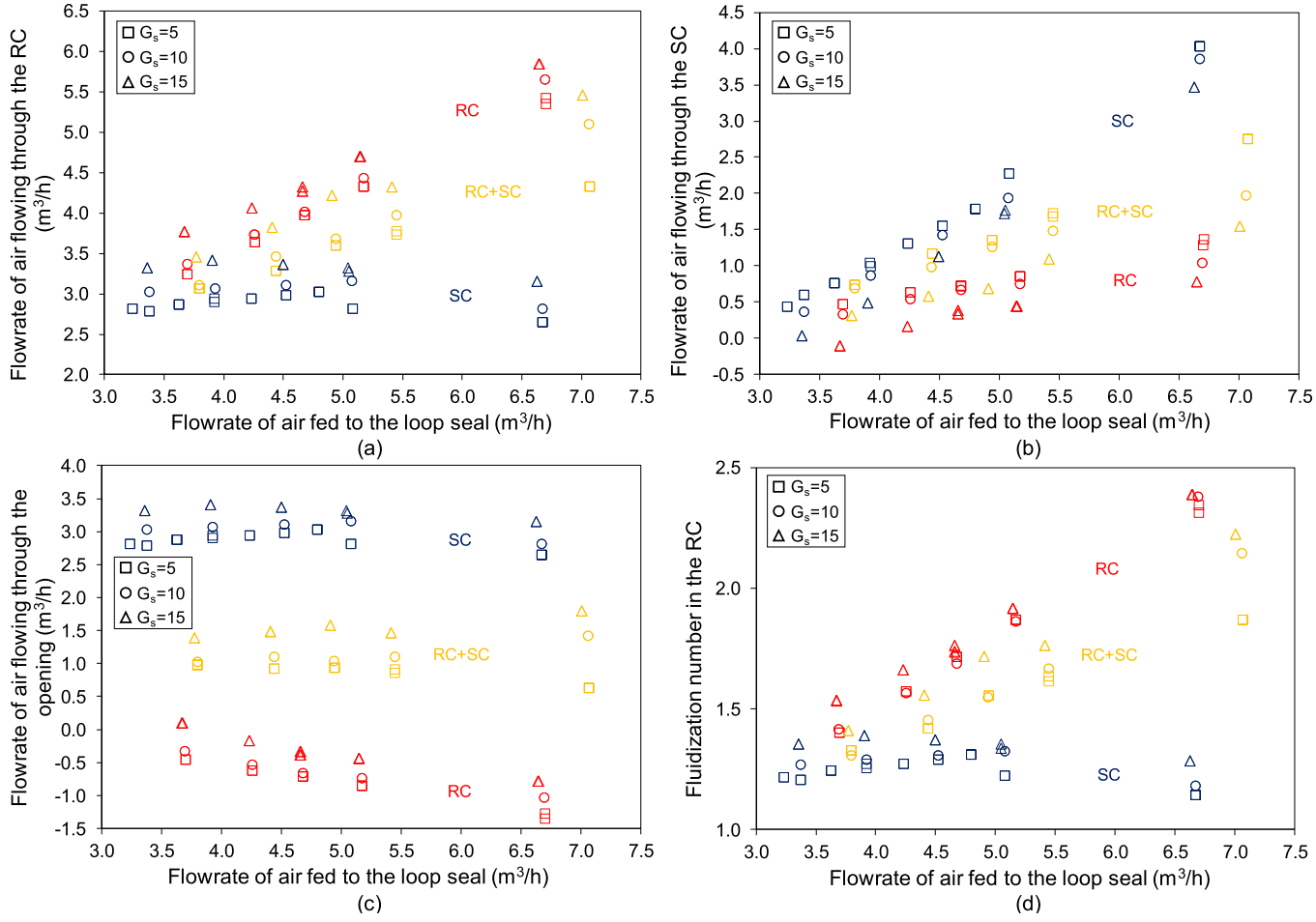

Fig. 4. Air flowing (a) through the RC, (b) SC and (c) opening, and (d) fluidization number in the RC (superficial gas velocity in the RC to minimum fluidization velocity considering the solids flux) against the total flowrate of air fed to the loop seal for tests with the outlet rotameter, under different solids fluxes (G_s: kg m^{-2} s^{-1}, referring to the cross section of the SC) and aeration modes (RC: only RC, RC + SC: both chambers, SC: only SC).

4.1. Experimental results

4.1.1. Tests with the outlet rotameter

The gas split between the chambers of the loop seal can be understood by examination of Fig. 4. The gas flowrate through the RC (Fig. 4(a)) and SC (Fig. 4(b)) is plotted as a function of the total flowrate fed into the loop seal for the three solids fluxes and three aeration modes investigated. In agreement with previous studies [16], the solids flux has a significant effect on the gas distribution. For a given aeration flowrate, the air flowing through the RC increases as the solids flux is increased, due to the higher amount of air dragged in the SC by the downwards flow of solids. Moreover, it can be observed that the increase in gas dragging is not linear but increases at higher solids fluxes. Both behaviors are observed for all the aeration modes.

Furthermore, it is seen that the gas split strongly depends on the aeration mode. For a given air flowrate fed to the loop seal, the highest gas flow through the RC is obtained when aerating through the RC, and the lowest by aerating through the SC. For a given solids flux, increasing the air flowrate through the SC leads to an almost constant gas flowrate through the RC. A considerable decrease is only observed when the SC gets fluidized, suggesting that once bubbles are formed in the SC, the gas finds lower resistance flowing through the bubbles than through the opening and the RC, resulting in a reduction of the gas circulation through the RC, even after increasing the total aeration. As expected, the flowrate of air at which the SC gets fluidized is higher as the solids flux is increased. When the loop seal is aerated through both chambers or through the RC, the air flowing through the RC always increases with the increase in the aeration flowrate.

Fig. 4(c) presents the flow of air circulating through the opening, which is defined as positive when circulating from the SC to the RC. It is observed that, for a given solids flux, when the loop seal is aerated through the SC and through both chambers, the gas flowrate through the opening is almost constant and positive for all the aeration flowrates tested. On the contrary, when the loop seal is aerated through the RC, the gas circulates from the RC to the SC (except for the lowest aeration flowrate at a solids flux of 15 kg m^{-2} s^{-1}, at which the gas is dragged from the SC to the RC) and it is higher as the air flowrate fed to the loop seal is increased.

During the tests it was observed that when aerating only through the SC, the RC was always a dense bed with no bubbles, while vigorous bubbling appeared as the gas flowrate was increased for the other aeration modes. This observation is evident from Fig. 4(d), where the fluidization number in the RC (ratio of actual to minimum fluidization velocity) is shown to be well below 1.5 and practically constant as the aeration increases through the SC, whereas it greatly increases when aerating through the RC. However, bubbles are expected to appear in the RC when aerating only through the SC at high enough solids fluxes as a result of the gas dragging (this was not observed in our experiments due to the limited range of solids fluxes tested).

A better understanding of the influence of aeration modes is obtained by analyzing Fig. 5 where the height of solids in the downcomer, the pressure at the bottom of the RC (tap 12) and that at the bottom of the SC (tap 10) are presented for the three aeration modes tested. The constriction introduced by the pressure drop of the valve prior to the

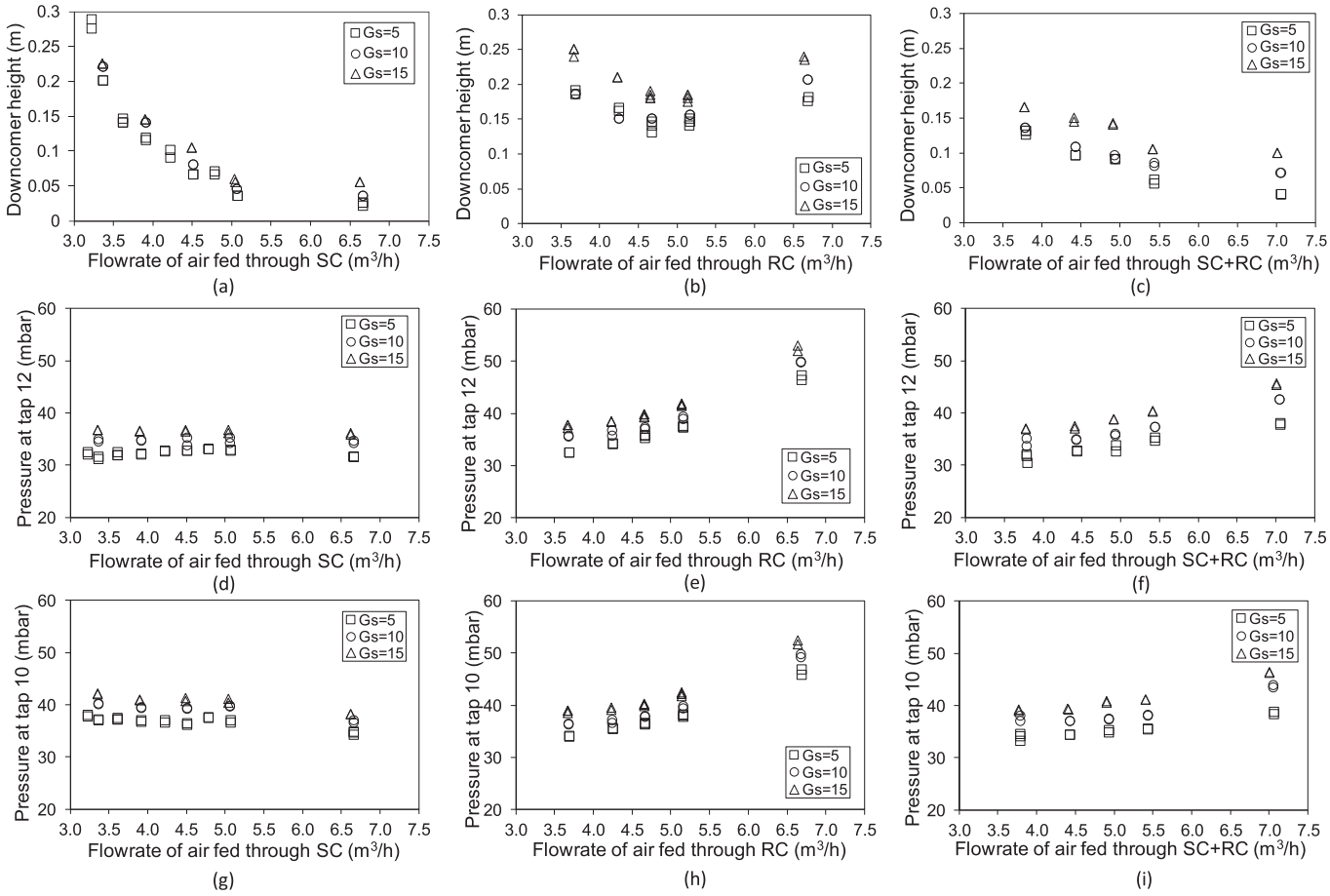

Fig. 5. Height of the downcomer (a, b, c) and pressure at taps 15 (d, e, f) and 10 (g, h, i) against the air fed through the different aeration modes for tests carried out with the outlet rotameter under the different solids fluxes (G_s: kg m^{-2} s^{-1}, referring to the cross section of the SC).

outlet rotameter needs to be considered when interpreting the experimental results from Fig. 5. Logically, the pressure drop through the valve is higher as the gas flowrate through the RC increases.

Fig. 5(a-c) shows that, for a given aeration, the increase in the solids flux increases the height of the downcomer, while, for a given solids flux, the height of the downcomer as the aeration increases, follows different patterns depending on the aeration mode. The height continuously decreases when the gas is fed through the SC and through both chambers (although not significantly), while it presents a minimum when aerating through the RC. These findings are discussed below.

When the loop seal is aerated through the SC, for a given solids flux, the amount of air flowing through the RC is almost constant (as shown in Fig. 4) leading to a fairly constant pressure drop in the outlet valve. As a result, the pressure is constant at the bottom of the RC (tap 12, Fig. 5(d)). The gas circulating through the SC increases consistently with the air flowrate fed to the SC, but the maximum pressure of the system does not change (tap 10, Fig. 5(g)). Therefore, the height of solids in the downcomer decreases, keeping the pressure constant while increasing the pressure gradient due to the higher relative velocity. It is also observed that the height of solids in the downcomer tends to a constant value at high gas flowrates since, once the SC gets fluidized, the pressure drop remains roughly constant with the air flowrate.

The aeration of the loop seal through the RC leads to the highest height of solids in the downcomer for a given flowrate of fed gas, as seen by comparison of Fig. 5(a) and Fig. 5(b). This is due to the lower gas flowing through the SC when aerating through the RC (Fig. 4(b)) (compared to the same aeration flowrate fed through the SC), which results in a higher height of solids to compensate for the pressure drop of the system. The height decreases with the increase in aeration flowrate through the RC, while the increase in the gas flow through the SC results in a higher pressure drop than that required to compensate for the pressure drop introduced by the outlet valve. For higher aerations, the pressure drop given by the outlet valve becomes so high that the increase in the gas flow through the SC is not enough to compensate for it and the column of solids starts building upwards, explaining the minimum found in Fig. 5(b).

It is notable that, in spite of the higher pressure at the bottom of the RC (at tap 12) when aerating through the RC, Fig. 5(e), (compared with that when aerating by the SC, Fig. 5(d)) caused by the higher pressure drop introduced by the outlet valve, it is observed that for low gas flowrates the pressure is lower at the bottom of the SC (Fig. 5(h)). The reason is that the pressure drop across the opening (P_{10}-P_{12}) is much lower when aerating through the RC (Fig. 6), compensating for the higher pressure drop given by the valve at low aerations.

As expected, an intermediate behavior is observed as the aeration is applied through both chambers. The height of solids in the downcomer (Fig. 5(c)) is in between that obtained for the SC and the RC aerations. The trend of the solids height profile is closer to that obtained when aerating through the SC since, for all the air flowrates tested, the circulation of gas through the SC led to a higher pressure drop than that required to compensate for the increase in pressure drop given by the outlet valve (leading to a decrease in the height of solids).

According to the measurements from the gas circulation through the opening (Fig. 4(c)) the behavior of pressure drop through it (P_{10}-P_{12}) could be anticipated a priori: (i) a rather constant pressure drop should be measured when aerating through the SC/both chambers (since the gas circulation is roughly independent of aeration flowrate for fixed solids flux), and (ii) a negative and decreasing pressure drop should be

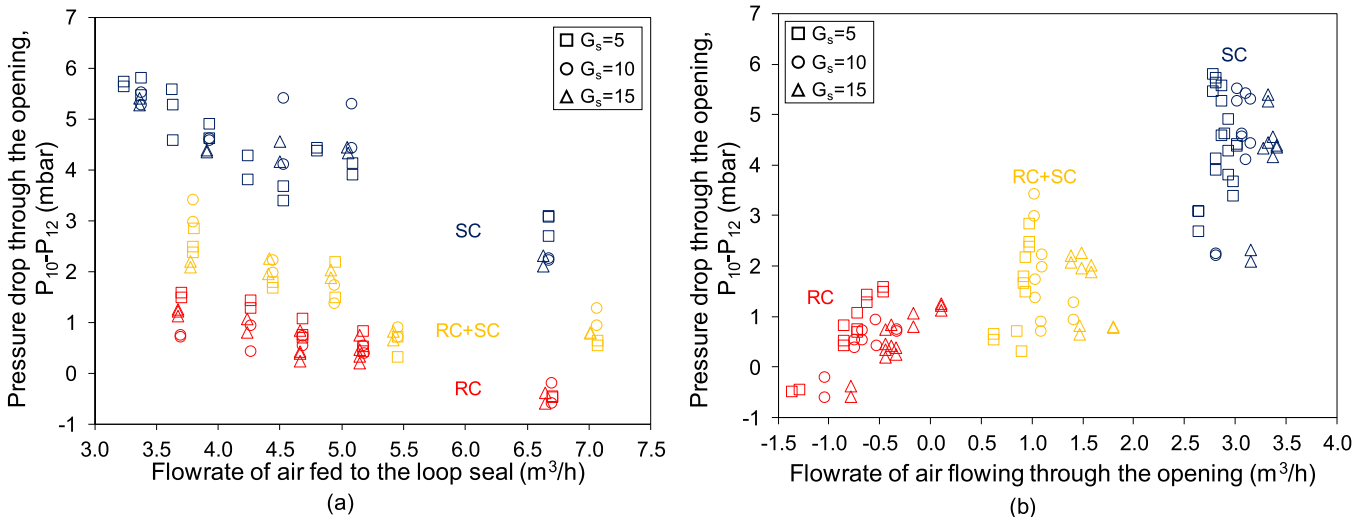

Fig. 6. Pressure drop through the opening against (a) the total flowrate of air fed to the loop seal and (b) the flowrate of air flowing through the opening for tests with the outlet rotameter under different solids fluxes (G_s: kg m^{-2} s^{-1}, referring to the cross section of the SC) and aeration modes (RC: only RC, RC + SC: both chambers, SC: only SC).

measured while increasing the aeration through the RC (since more gas circulates from 12 to 10). However, as shown in Fig. 6, where the pressure drop measured across the opening is plotted as a function of the aeration flowrate (Fig. 6(a)) and of the actual gas flowing through the opening (Fig. 6(b)), the actual behavior apparently differs from that expected. Despite the scattering of measurements, it is clearly seen that the pressure drop is higher when aerating through the SC and it decreases, for the three aeration modes, with the increase in the aeration flowrate to the loop seal. The latter contradicts statement (i). However, it can be explained by considering the irregular gas-solid flow through the opening. At low aerations the solids at the bottom of the SC are very compacted, favoring gas shortcuts instead of a homogenous distribution. As the aeration is increased, the solids are softened, allowing for a better distribution of the gas through the cross section of the horizontal passage and the opening. When taking a shortcut, a given gas flowrate through the opening leads to higher pressure drop due to the higher gas-solids relative velocity (narrower effective cross section). The same gas flowrate under a homogeneous gas-solid flow distribution leads to lower gas-solids relative velocity resulting in lower pressure drop. Finally, it is observed that the trend of the pressure drop with the aeration through the RC is consistent with that expected in statement (ii), although the expected negative pressure drops were only registered for the highest air flowrate tested.

The ability of the different aeration modes to change the solids flux in a CFB unit is assessed in this work through the increase in the standpipe pressure gradient (see Section 4.2.1 for details on the operation of loop seals in CFB systems). This increase in the pressure gradient is evaluated by the change in the pressure drop measured between taps 10–8, which are always covered by solids. Measurements reported in Fig. 7(a) show that the pressure gradient through the SC increases for all the aeration modes but the highest slope is observed when aerating only through the SC. This implies that, in a CFB unit, the aeration of the loop seal through the SC allows for controlling of the solids circulation with the lowest aeration and solids inventory. The maximum solids flux given by the

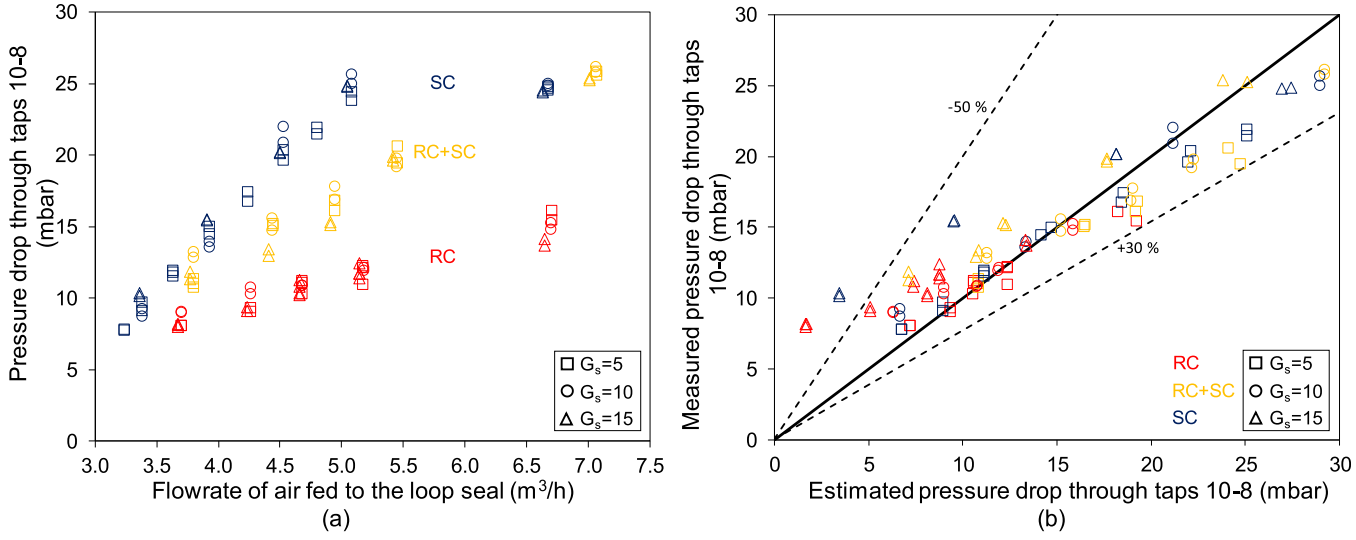

Fig. 7. Pressure drop through the SC between taps 10–8 against the flowrate of air fed to the loop seal (a) and measured (Exp.) and estimated (Est.) pressure drop through the SC between taps 10–8 against the superficial gas-solids relative velocity in the supply chamber (b) for tests with the outlet rotameter under different solids fluxes (G_s: kg m^{-2} s^{-1}, referring to the cross section of the SC) and aeration modes (RC: only RC, RC + SC: both chambers, SC: only SC), only tests with the SC under moving bed regime are considered in (b).

loop seal operated as a non-mechanical valve is that of the SC under fluidized regime (from this point forward there is no change in the pressure drop of the SC/downcomer), which is reached at approximately 5 m^3/s when aerating through the SC and 7 m^3/s when aerating through both chambers while, for the flowrates of air tested, it is never reached when feeding the air through the RC.

As a way to assess the quality of the gas distribution across the SC, the pressure drop between taps 10–8 have been estimated using the Ergun equation (Eq. (5)), assuming a constant bed voidage equal to that at incipient fluidization, for tests with a gas-solids relative velocity below that of minimum fluidization. Results are presented in Fig. 7(b) where high discrepancies are observed for the lowest pressures, corresponding to those tests in which the gas is not well-distributed across the section of the SC. This is consistent with the explanations provided above: the gas short-cuts the bed at low gas flows, passing through a narrower section than that of the SC, which results in a higher pressure drop compared to that estimated from the Ergun equation. A comprehensive qualitative analysis of the misdistribution of gas and solids in the loop seal operation is given in Section 4.1.3.

4.1.2. Comparison of tests with and without the outlet rotameter

Tests without the outlet rotameter were conducted to compare the performance of the loop seal with and without restriction to flow at the exit of the RC (i.e., the difference of pressure drop (P_{15}-P_1)). As the gas distribution cannot be directly measured in tests without the outlet rotameter, the comparison is made qualitatively through the height of solids in the downcomer and the pressure drops throughout the system, for the same operating conditions (aeration mode and flowrate).

In tests without the outlet valve, the maximum pressure of the isolated loop seal rig (that of tap 10 or 12, depending on the operating conditions) either remains constant or slightly decreases (due to the RC bed expansion) as the gas flowrate fed to the loop seal is increased, but it never increases as it does when operating with the outlet valve. As a result, the height of solids in the downcomer always decreases with the air flowrate, even for the aeration through the RC (Fig. 8) (in contrast to the increase observed in the operation with the outlet rotameter to compensate for the high pressure drop given by the outlet valve). Moreover, as expected, a lower level is reached by solids in the downcomer in tests carried out without the outlet valve. The highest difference in heights is observed for tests aerated through the RC as are those, in tests with the outlet rotameter, with the highest circulation of gas through the RC, leading to a higher pressure drop at the outlet valve (represented by pressure at tap 15, Fig. 9(a)).

Fig. 9(a-c) compares the pressure drop through the RC, the SC and the opening for tests with and without the outlet valve and a solids flux of 5 kg m^{-2} s^{-1}. The pressure drop through the RC (represented by pressure drop 12–13 in Fig. 9(b)) tends to be lower in tests without the outlet valve due to bed expansion, consistently with a higher flowrate of gas through the RC. This behavior is more prevalent in tests carried out for a solids flux of 15 kg m^{-2} s^{-1} (not reported here) where more gas flows through the RC due to the solids dragging. The pressure drop in the SC cannot be assessed so easily since it also depends on the pressure drop across the opening, which is difficult to evaluate. Although accurate estimations of the gas distribution along the loop seal are not possible in tests without the outlet rotameter, it is clear from Fig. 9 that the performance of the loop seal follows the same trends with and without the outlet valve. The conclusion is that, although the actual gas-solids distribution is affected by the pressure drop along the other components of the CFB loop, the pattern of the resistance of the loop seal unit to gas-solids flow (resistance curve) is characterized, to a large extent, by its geometry.

4.1.3. Implications of gas-solids flow patterns in the operation and modeling of loop seals

The above experimental results showed that the aeration mode, together with the geometry of the unit, establishes the distribution of the gas fed through the loop seal and, therefore, the performance of the loop seal under different aeration and solids flowrates. It was also demonstrated that the non-homogeneous gas distribution and the presence of stagnant zones of solids are essential to understand (and to predict) the gas split between the chambers.

Fig. 10 and Fig. 11 show a representation of the non-ideal gas and solids flow patterns observed when operating the loop seal under mono-chamber aerations, SC and RC, respectively. The stagnant zone formed at the bottom of the SC is reduced with the increase in aeration through the SC until disappearing once it becomes fluidized Fig. 10(a-c). At low solids flows the RC is a dense bed close to incipient fluidization, while bubbles start flowing close to the central baffle as the solids flow is increased, due to the higher contribution of the gas dragged by solids (Fig. 10(d)). Although not represented in figures, it is clear from Fig. 10 (d) that when aerating through the SC the gas is spread into the RC through the upper part of the opening, leading to a lower stagnant zone in the RC. Fig. 11 shows that the operation of the loop seal when aerated through the RC is characterized by a huge stagnant zone in the SC, but good gas distribution across the RC, leading to vigorous bubbling as the aeration is increased. Although the death zone in the SC gets smaller both with increasing the aeration and the solids circulation, it always remains sizable (Fig. 11(c)). An intermediate behavior is obtained when

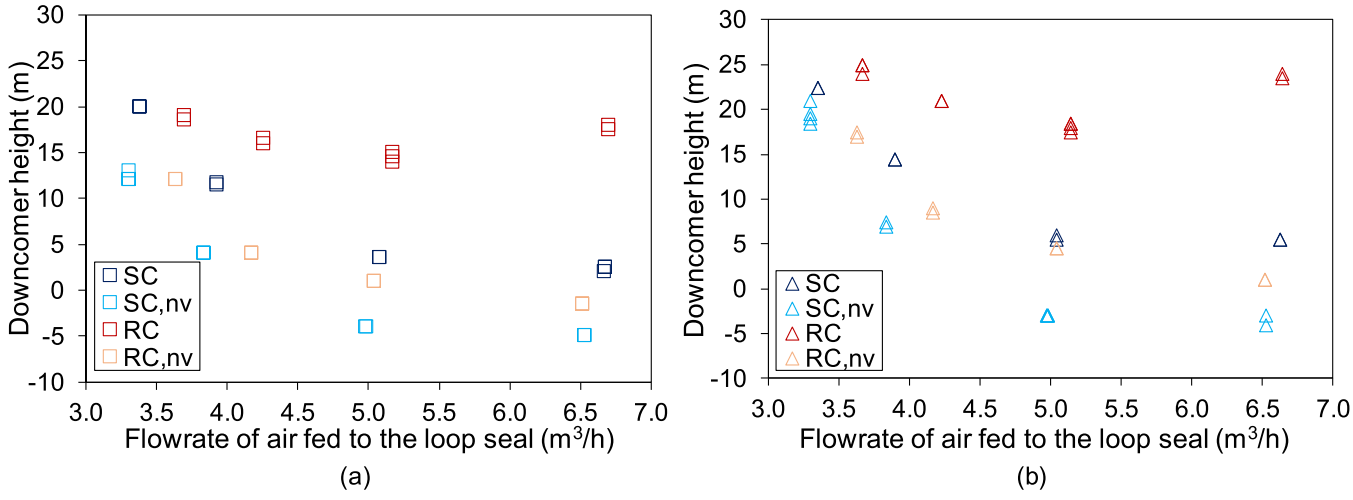

Fig. 8. Downcomer height against the flowrate of air fed to the loop seal for tests carried out with and without the outlet rotameter (nv), under different aeration modes (RC: only RC, SC: only SC) and solids flux (G_s: kg m^{-2} s^{-1}, referring to the cross section of the SC) of 5 (a) and 15 (b).

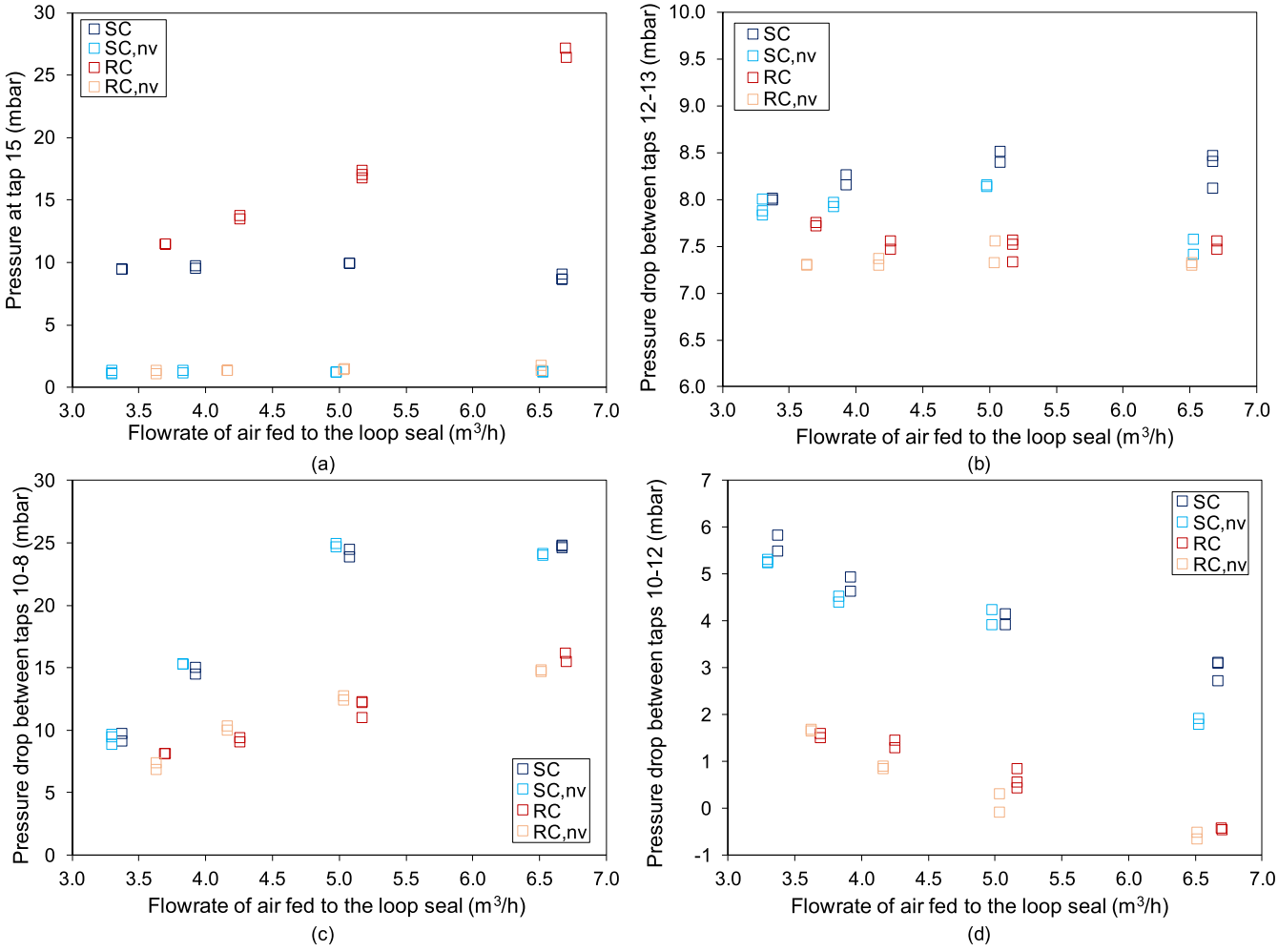

Fig. 9. Pressure at tap 15 (a) and pressure drop through the RC between taps 12–13 (b), through the SC between taps 10–8 (c) and through the opening between taps 10–12 (d) against the flowrate of air fed to the loop seal for tests carried out with and without the outlet valve (nv), under different aeration modes (RC: only RC, SC: only SC) and a solids flux of 5 (G_s: kg m^{-2} s^{-1}, referring to the cross section of the SC).

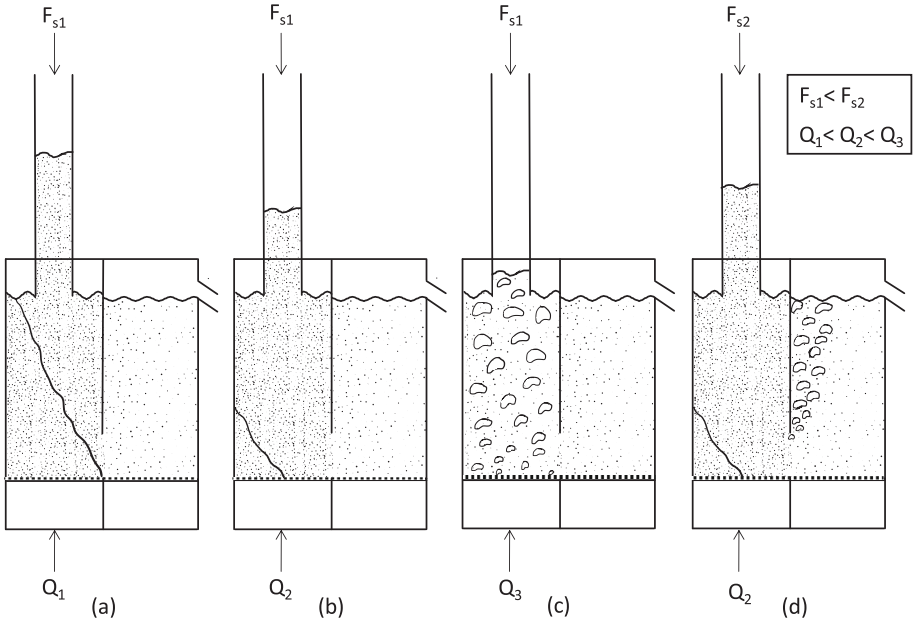

Fig. 10. Gas and solids flow patterns when aerating through the supply chamber for different aeration rates (Q_1, Q_2 and Q_3) and different solids flows (F_{s1} and F_{s2}).

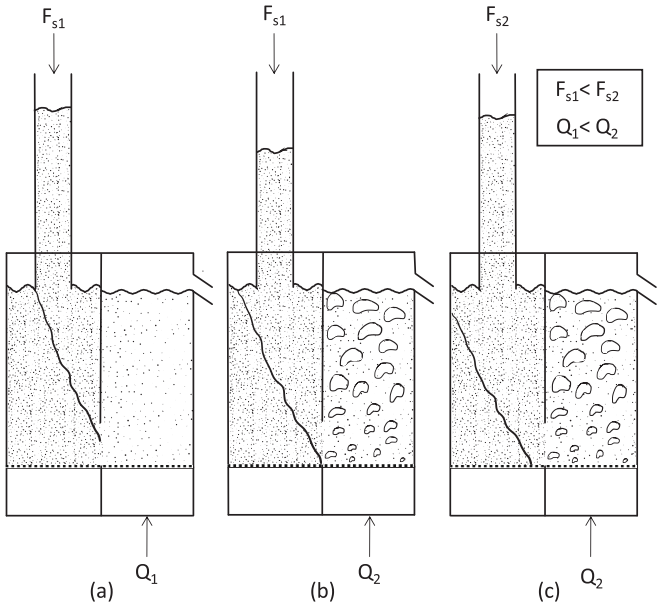

Fig. 11. Gas and solids flow patterns when aerating through the recycle chamber for different aeration rates (Q_1 and Q_2) and different solids flows (F_{s1} and F_{s2}).

aerating the loop seal through both chambers. The evolution of the stagnant zone in the SC of a loop seal equally aerated under both chambers was assessed in [18] using tracer solids, confirming our observations and measurements.

It is concluded that, regardless of the aeration mode, there is always a stagnant zone in the SC when operated under moving bed flow. The size of the stagnant zone is reduced as the air and solids flows increase, but it only disappears when the SC gets fluidized (which only happens at high aeration rates fed through the SC); at this aeration point, the loop seal loses the ability to control the solids circulation. In other words, the operation of a loop seal as a non-mechanical valve always entails the presence of a death zone in the SC. On the contrary, stagnancies in the RC can be easily avoided by providing some aeration through the RC.

The unexpected trends found when analyzing the pressure drop through the opening (Fig. 6) are the result of the particular features of the gas-solids flows across the loop seal. It was demonstrated that the pressure drop through the opening is affected by the aeration mode and it does not follow a homogeneous gas-solids pattern. As a result, this pressure drop cannot be estimated as that between two fluidized beds [41], which is assumed by many authors [21,27]. Special features concerning the gas-solids flow through the opening in a loop seal unit are extensively assessed in [13].

The superior performance of the loop seal for controlling the solids circulation in a CFB loop when aerated through the SC (Fig. 7(a) and Fig. 9(c)) is achieved due to the high resistance offered by the opening which, for a given aeration, leads to a higher circulation of gas through the SC. Feeding the same air flowrate through the RC leads to the lowest circulation of gas through the SC i.e., the lowest pressure drop and solids circulation. The best option when the stagnant zones are to be minimized is the aeration through both the SC and RC. If the loop seal is intended just as a solids circulation device, aerating through both chambers while keeping the SC under fluidized regime is the best option to reach the maximum solids flux, promoting a uniform and smoother gas-solids flow (see Section 4.2.1 for details on the operation of loop seals in CFB systems). It can be concluded that the lower the stagnant zones and gas-solids flow resistances the lower the loop seal ability to control the solids circulation in a CFB loop.

A proper model of the resistance to flow found by gas and solids in actual loop seals (as a function of the aeration) would allow for the solution of the model presented in Section 2.2. Special attention needs to be paid to the opening/horizontal passage, usually not considered in models [10,37,38,40], since it tends to be the limiting resistance, establishing the gas and solids distribution in a loop seal device. Unfortunately, non-ideal gas-solids flow patterns occurring in actual loop seals cannot be addressed by simple semi-empirical 1D models. This explains why the models of loop seal in CFB and DFB are still generally based on empirical correlations, which are difficult to apply outside of the system in which they were obtained. To obtain a comprehensive description, CFD simulation appears to be the best way to predict the actual gas-solid flow if a new loop seal is to be designed. However, modeling of the gas-solid flow in the loop seal and the standpipe is still recognized as the bottleneck for the simulations of the whole CFB loop in the CFD scheme [46,47].

4.2. Loop seal coupled to a CFB unit

4.2.1. Control of solids circulation in a CFB unit

The pressure balance of a typical CFB unit, as that sketched in Fig. 12, is given by Eq. (14) where the pressure drop through the connection in between the RC and the riser has been neglected. Eq. (14) shows that the pressure drop given by the column of solids in the standpipe balances the pressure of the rest of the system.

$$\Delta P_{SP} = \Delta P_{OP} + \Delta P_{RC} + \Delta P_R + \Delta P_{CY} \tag{14}$$

There are two statements that must be fulfilled at any CFB unit in which the solids circulation is intended to be controlled by the aeration in the loop seal (Fig. 12)

$$\frac{\partial \Delta P_{SP}}{\partial Q_{LS}} > 0$$

$$\left.\frac{\partial G_s}{\partial \Delta P_R}\right|_{Q_R} > 0$$

meaning that, (i) the standpipe must be operated under moving bed flow and (ii) the entrainment in the riser should be sensitive to the solids inventory in the riser, i.e., from a design point of view:

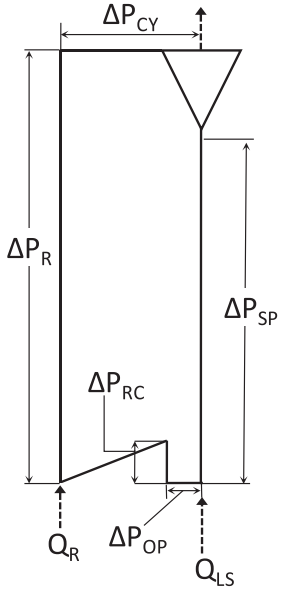

Fig. 12. Sketch of the pressure loop through a CFB unit (Q_R: flowrate of gas fed to the riser; Q_{LS}: flowrate of gas fed to the loop seal).

- The cross section of the standpipe must be selected to allow that the superficial velocity of the solids, under the maximum operating solids flux, is lower than that of incipient fluidization.
- The riser must be designed to operate below the saturation carrying capacity of the gas, considering the operative window of gas and solids velocities.

If any of these requirements is not fulfilled, the loop seal will never be able to control the solids flux. In typical CFB boilers these requirements are rarely met since the huge solids circulations implies solids velocities in the standpipes above that of incipient fluidization. Moreover, in CFB boilers the height of the riser is to be maximized for allocating the water walls, hence the widespread belief in the boiler community regarding the limited ability of loop seals for controlling the solids circulation.

For a given aeration in the riser, as increasing the aeration in the loop seal, the gradient of pressure in the standpipe increases and the height of solids decreases due to the evacuation of material, which accumulates in the riser, satisfying the new pressure balance (Eq. (14)). If the riser is operated below the saturating carrying capacity, the solids flux increases with the increase in the solids inventory and pressure drop in the riser; otherwise, the system reaches a new steady state with the same solids circulation but higher pressure. If the aeration in the loop seal is such that the standpipe is fluidized, the system operates with the minimum height of solids in the standpipe, maximum sealing pressure, maximum solids inventory in the riser, and consequently, maximum solids circulation. Under this operation, the resistance in the circulating device is minimum and the solids circulation can only be increased by increasing the aeration in the riser. In a properly designed CFB unit the widest range of solids circulation control is obtained when combining both the loop seal and riser aerations.

4.2.2. *Extrapolating the performance of an isolated loop seal to one operating within a CFB unit*

As shown in the previous section, in a CFB unit the performance of the loop seal is subjected to that of the whole system. Hence, for a given set of operating conditions (Q_R, Q_{LS} and solids inventory), the system evolves leading to the solids circulation and the solids distribution around the loop which satisfy the pressure balance according to Eq. (14).

Note that in an isolated loop seal, such as that used in this study (Fig. 3), setting a solids flux, G_s, and an aeration flowrate, Q_{LS}, the height of solids in the downcomer (i.e., solids inventory) and the pressure drop in the outlet valve, ΔP_{OV} (P_{15}-P_1, according to Fig. 3) are established. The pressure balance for the isolated system is,

$$\Delta P_{SP} = \Delta P_{OP} + \Delta P_{RC} + \Delta P_{OV} \quad (15)$$

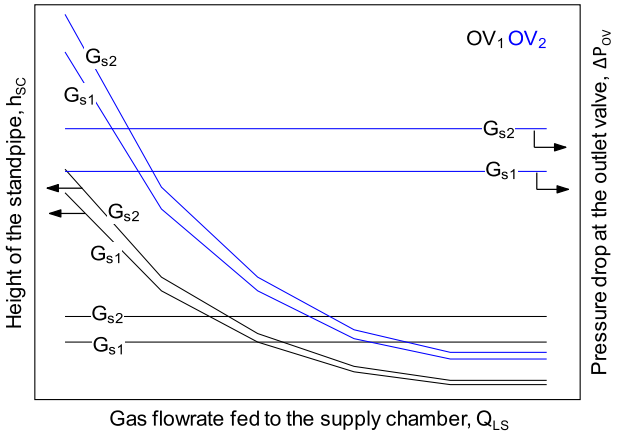

Fig. 13. Qualitative operational map of an isolated loop seal aerated through the SC under different solids fluxes ($G_{s1} < G_{s2}$) and apertures of the outlet valve (OV_1 representing a higher aperture of the outlet valve, compared to OV_2).

Comparing the pressure balance of a given isolated loop seal (Eq. (15)) with the same loopseal coupled to a riser in a CFB unit (Eq. (14)), it holds,

$$\Delta P_{OV} = \Delta P_R + \Delta P_{CY} \quad (16)$$

which means that the performance of an isolated loop seal under a given Q_{LS} and G_s, can represent the operation of the same loop seal unit coupled to a CFB system operating under the same G_s and, in which the pressure drop of the riser and the cyclone is equal to ΔP_{OV}.

The performance of the isolated loop seal can be characterized by making a performance chart such as that qualitatively represented in Fig. 13. This chart corresponds to the operation of a loop seal rig when aerated through the SC: varying G_s, Q_{LS} and the aperture of the outlet valve, *OV,* and registering the height of the SC, h_{SC}, and the pressure drop in the outlet valve, ΔP_{OV}. The chart can be used to obtain the aeration required in that loop seal when coupled to a CFB unit to achieve a given solids flux. This is done by entering with the required G_s, the pressure drop given by the riser and the cyclone of the CFB for G_s (ΔP_{OV}), and the solids inventory in the standpipe (which can be converted into h_{SC}). The solids inventory in the standpipe can be roughly obtained by deducting from the total solids inventory in the operation, that required in the riser to give G_s at the riser velocity. Finally, the analysis can also provide the maximum pressure drop sealed by a given loop seal, which corresponds to the solids flux that leads to the maximum height of solids (geometrically allowed) in the downcomer under fluidized flow (i.e., high aeration).

5. Conclusions

The gas distribution along the loop seal is the key issue determining the performance of loop seals as non-mechanical valves. Despite the great effort made to understand and model the gas split in a loop seal device, a review of previous works has shown that this issue is controversial and there are contradictory results. Therefore, there is not yet a comprehensive method to calculate the gas-solid flow in a loop seal of a CFB. Dedicated experiments were conducted in this work to shed light on these issues. Experimental work was conducted in an isolated loop seal and the gas distribution was assessed through direct measurement of the gas flow leaving the recycle chamber (RC) under different modes of aeration (only supply chamber, SC, only RC and both chambers), aeration flowrates and solids fluxes. The main conclusions obtained from the study are:

- The aeration mode and the geometry of the unit have a huge effect on the gas distribution in a loop seal.
- The aeration through the SC allows the highest solids flux at the lowest aeration flowrate, while aeration through the RC leads to the lowest solids flux; aerating through both chambers leads to an intermediate solids flux and a smoother operation.
- The resistance offered by the horizontal passage (opening) joining the bottom of the SC and RC results in a non-homogeneous gas-solids flow pattern which, ultimately, establishes the actual gas division through the chambers.
- Non-ideal gas-solids flow patterns occurring in actual loop seals cannot be addressed by simple semi-empirical 1D models; although CFD appears a useful tool to predict the behavior of these units, a comprehensive generalization is difficult.
- A method for characterizing the operation of an isolated loop seal in operational maps that can be used afterwards to couple the loop seal within a CFB unit was proposed.

The knowledge gained in this study gives a general view of the performance of a typical loop seal unit. Similar performances are expected from geometrically similar loop seals and, although industrial loop seals tend to have longer horizontal channels leading to higher

resistances to gas-solids flow, the general conclusions from this study still stand.

Nomenclature

A	cross section, m^2
d_p	particle size, m
F_s	solids flow, kg s^{-1}
g	gravitational acceleration, m s^{-2}
G_s	solids flux (generally referred to the riser; in the experiments to the SC), kg m^{-2} s^{-1}
h	height, m
P	pressure, Pa
Q	gas flowrate, m^3 s-1
u_0	superficial gas velocity, m s^{-1}
u_g	actual gas velocity, m s^{-1}
u_{mf}	minimum fluidization velocity, m s^{-1}
u_s	solids velocity, m s^{-1}

Greek symbols

δ	bubble fraction, –
ΔP	pressure drop, Pa
ε	voidage, –
μ_g	viscosity of the gas, kg m^{-1} s^{-1}
ρ	density, kg m^{-3}
Φ	particle sphericity, –

Subscripts

CY	cyclone
g	referring to the gas
LS	loop seal
mf	minimum fluidization
nv	no valve, referring to tests carried out without outlet valve
OP	opening
OV	outlet valve
p	referring to the particle
R	riser
x	referring to pressure at the inlet of the SC
y	referring to pressure at the outlet of the RC

Abbreviations

1D	one-dimensional
CFB	circulating fluidized bed
CFD	computational fluid dynamics
DFB	dual fluidized bed
RC	recycle chamber
SC	supply chamber

CRediT authorship contribution statement

M. Suárez-Almeida: Investigation, Conceptualization, Methodology, Data curation, Formal analysis, Writing – original draft, Visualization. **A. Gómez-Barea:** Conceptualization, Methodology, Formal analysis, Resources, Funding acquisition, Project administration, Supervision, Writing – review & editing.

Declaration of Competing Interest

The authors declare that they have no known competing financial interests or personal relationships that could have appeared to influence the work reported in this paper.

Acknowledgements

This work was supported by the Spanish National Plan I+D+i (Project PID2020-117794-RB), by Junta de Andalucía through the project P18-RT-4512 (co-funded by European Regional Development Fund/European Social Fund "A way to make Europe") and, by Ministerio de Economía, Industria y Competitividad of the Spanish government under the call "Ayudas para Contratos Predoctorales 2017" financed together FSE with the PhD grant (BES-2017-080653).

References

[1] P. Basu, Solid recycle systems, in: Combust. Gasif. Fluid. Beds, 1 st., CRC Press, 2006, pp. 417–437, https://doi.org/10.1201/9781420005158.ch13.
[2] T. Knowlton, Standpipes and nonmechanical valves, in: W.-C. Yang (Ed.), Handb. Fluid. Fluid-Particle Syst, 1 st, CRC Press, 2003, https://doi.org/10.1201/9780203912744.ch21.
[3] X. Han, Z. Cui, X. Jiang, J. Liu, Regulating characteristics of loop seal in a 65 t/h oil shale-fired circulating fluidized bed boiler, Powder Technol. 178 (2007) 114–118, https://doi.org/10.1016/j.powtec.2007.04.015.
[4] P. Basu, M. Chandel, J. Butler, A. Dutta, An investigation into the operation of the twin-exit loop-seal of a circulating fluidized bed boiler in a thermal power plant and its design implication, J. Energy Resour. Technol. Trans. ASME. 131 (2009) 0414011–0414018, https://doi.org/10.1115/1.4000174.
[5] X. Ji, X. Lu, H. He, J. Lu, Q. Wang, Y. Kang, L. Yan, Study on the gas-solid flow and heat transfer characteristics of evaporating recycle valve, Powder Technol. 228 (2012) 219–227, https://doi.org/10.1016/j.powtec.2012.05.019.
[6] E.R. Monazam, L.J. Shadle, J.S. Mei, Impact of the circulating fluidized bed riser on the performance of a loopseal nonmechanical valve, Ind. Eng. Chem. Res. 46 (2007) 1843–1850, https://doi.org/10.1021/ie0606486.
[7] M. Stollhof, S. Penthor, K. Mayer, H. Hofbauer, Influence of the loop seal fluidization on the operation of a fluidized bed reactor system, Powder Technol. 352 (2019) 422–435, https://doi.org/10.1016/j.powtec.2019.04.081.
[8] A. Johansson, F. Johnsson, B.Å. Andersson, The performance of a loop seal in a CFB boiler, J. Energy Resour. Technol. Trans. ASME. 128 (2006) 135–141, https://doi.org/10.1115/1.2199567.
[9] M. Kolbitsch, First Fuel Tests at a Novel 100 kWth Dual Fluidized Bed Steam Gasification Pilot Plant, Vienna University of Technology, 2016.
[10] M. Suárez-Almeida, A. Gómez-Barea, C. Pfeifer, B. Leckner, Fluid dynamic analysis of dual fluidized bed gasifier for solar applications, Powder Technol. 390 (2021) 482–495, https://doi.org/10.1016/j.powtec.2021.05.032.
[11] Y.A. Criado, M. Alonso, J.C. Abanades, Z. Anxionnaz-Minvielle, Conceptual process design of a CaO/Ca(OH)2thermochemical energy storage system using fluidized bed reactors, Appl. Therm. Eng. 73 (2014) 1087–1094, https://doi.org/10.1016/j.applthermaleng.2014.08.065.
[12] S.W. Kim, S.D. Kim, Effects of particle properties on solids recycle in loop-seal of a circulating fluidized bed, Powder Technol. 124 (2002) 76–84, https://doi.org/10.1016/S0032-5910(01)00472-7.
[13] P. Basu, J. Butler, Studies on the operation of loop-seal in circulating fluidized bed boilers, Appl. Energy 86 (2009) 1723–1731, https://doi.org/10.1016/j.apenergy.2008.11.024.
[14] A.R. Bidwe, A. Charitos, H. Dieter, A. Wei, M. Zieba, A study of standpipe and loop seal behaviour in a circulating fluidized bed for Geldart B particles, Proc. Tenth Intenational Conferance Circ. Fluid. Beds Fluid. Technol. CFB 10 (2011) 641–648.
[15] P. Wang, J. Lu, W. Xing, H. Yang, M. Zhang, Impact of loop seal structure on gas solid flow in a CFB system, Powder Technol. 264 (2014) 177–183, https://doi.org/10.1016/j.powtec.2014.04.037.
[16] Y. Li, Y. Lu, F. Wang, K. Han, W. Mi, X. Chen, P. Wang, Behavior of gas-solid flow in the downcomer of a circulating fluidized bed reactor with a V-valve, Powder Technol. 91 (1997) 11–16, https://doi.org/10.1016/S0032-5910(96)03226-3.
[17] X. Yao, H. Yang, H. Zhang, C. Zhou, Q. Liu, G. Yue, Gas-solid flow behavior in the standpipe of a circulating fluidized bed with a loop seal, Energy and Fuels. 25 (2011) 246–250, https://doi.org/10.1021/ef1011897.
[18] P. Bareschino, R. Solimene, R. Chirone, P. Salatino, Gas and solid flow patterns in the loop-seal of a circulating fluidized bed, Powder Technol. 264 (2014) 197–202, https://doi.org/10.1016/j.powtec.2014.05.036.
[19] M.M. Yazdanpanah, A. Forret, T. Gauthier, A. Delebarre, An experimental investigation of loop-seal operation in an interconnected circulating fluidized bed system, Powder Technol. 237 (2013) 266–275, https://doi.org/10.1016/j.powtec.2012.11.033.
[20] E. Johansson, A. Lyngfelt, T. Mattisson, F. Johnsson, Gas leakage measurements in a cold model of an interconnected fluidized bed for chemical-looping combustion, Powder Technol. 134 (2003) 210–217, https://doi.org/10.1016/S0032-5910(03)00125-6.
[21] L. Cheng, P. Basu, Effect of pressure on loop seal operation for a pressurized circulating fluidized bed, Powder Technol. 103 (1999) 203–211, https://doi.org/10.1016/S0032-5910(99)00018-2.
[22] P. Basu, Z. Luo, M. Boyd, L. Cheng, K. Cen, An experimental investigation into a loopseal in a circulating fluidized bed, in: Circ. Fluid. Bed Technol. VI, Wuerzburg, 1999, pp. 805–810.

[23] S. Yang, H. Yang, H. Zhang, J. Li, G. Yue, Impact of operating conditions on the performance of the external loop in a CFB reactor, Chem. Eng. Process. Process Intensif. 48 (2009) 921–926, https://doi.org/10.1016/j.cep.2008.12.004.
[24] F. Oliveira, G.H. Santos Furquim, V.O. Ochoski Machado, M.R. Parise, J., Ramírez Bahainne, operational influence of the mono-chamber aeration mode in the loop seal of a circulating fluidized bed, Lat. Am. Appl. Res. 51 (2021) 15–20, https://doi.org/10.52292/j.laar.2021.181.
[25] M.W. Seo, T.D.B. Nguyen, Y. Il Lim, S.D. Kim, S. Park, B.H. Song, Y.J. Kim, Solid circulation and loop-seal characteristics of a dual circulating fluidized bed: experiments and CFD simulation, Chem. Eng. J. 168 (2011) 803–811, https://doi.org/10.1016/j.cej.2011.01.041.
[26] P. Basu, Circulating Fluidized Bed Boilers Design, Operation and Maintenance, Springer, 2015, pp. 229–253, https://doi.org/10.1007/978-3-319-06173-3.
[27] P. Gao, Z. Tang, Y. Han, E. Li, X. Zhang, A pressure drop model of U-typed reduction chamber for iron ore suspension roasting, Powder Technol. 343 (2019) 255–261, https://doi.org/10.1016/j.powtec.2018.11.020.
[28] Z. Tang, P. Gao, Y. Sun, Y. Han, Experimental study on fluidization characteristics of different-sized particles in a U-type reduction chamber 30, 2019, pp. 2430–2439.
[29] S.W. Kim, W. Namkung, S.D. Kim, Solid recycle characteristics of loop-seals in a circulating fluidized bed, Chem. Eng. Technol. 24 (2001) 843–849, https://doi.org/10.1002/1521-4125(200108)24:8<843::AID-CEAT843>3.0.CO;2-D.
[30] S.W. Kim, W. Namkung, S.D. Kim, Solids flow characteristics in loop-seal of a circulating fluidized bed, Korean J. Chem. Eng. 16 (1999) 82–88, https://doi.org/10.1007/BF02699009.
[31] W. Namkung, M. Cho, Loop-seal operation of iron ore particles in pneumatic conveying, Korean J. Chem. Eng. 19 (2002) 1066–1071.
[32] A. Chinsuwan, J. Somjun, An investigation of performance of a conventional U type loop-seal for CFB reactors with side and bottom aerations, Chem. Eng. Res. Des. 3 (2020) 58–66, https://doi.org/10.1016/j.cherd.2020.08.013.
[33] A. Armatsombat, A. Chinsuwan, An Investigation of Characteristics of a Loop Seal with and without Side Aeration, 2018, pp. 117–120.
[34] F. Johnsson, S. Andersson, B. Leckner, Expansion of a freely bubbling fluidized bed, Powder Technol. 68 (1991) 117–123, https://doi.org/10.1016/0032-5910(91)80118-3.
[35] D. Kunii, O. Levenspiel, Fluidization Engineering, 2nd ed, Butterworth-Heinemann, Stoneham, 1992, https://doi.org/10.1016/b978-0-7506-9236-6.50001-9.
[36] E. Botsio, P. Basu, Experimental investigation into the hydrodynamics of flow of solids through a loop seal recycle chamber, Can. J. Chem. Eng. 83 (2005) 554–558, https://doi.org/10.1002/cjce.5450830319.
[37] C. Li, H. Li, Q. Zhu, A hydrodynamic model of loop-seal for a circulating fluidized bed, Powder Technol. 252 (2014) 14–19, https://doi.org/10.1016/j.powtec.2013.10.029.
[38] C. Li, Z. Zou, H. Li, Q. Zhu, A hydrodynamic model of loop seal with a fluidized standpipe for a circulating fluidized bed, Particuology. 36 (2018) 50–58, https://doi.org/10.1016/j.partic.2017.02.005.
[39] C.M. Eleftheriades, M.R. Judd, The design of downcomers joining gas-fluidized beds in multistage systems, Powder Technol. 21 (1978) 217–225, https://doi.org/10.1016/0032-5910(78)80091-6.
[40] Z. Tang, Y. Han, P. Gao, F. Yang, K. Xu, Y. Feng, A hydrodynamic model of U-type reduction chamber for iron ore suspension roaster, Powder Technol. 393 (2021) 441–448, https://doi.org/10.1016/j.powtec.2021.08.004.
[41] M. Kuramoto, D. Kunii, T. Furusawa, Flow of dense fluidized particles through an opening in a circulation system, Powder Technol. 47 (1986) 141–149, https://doi.org/10.1016/0032-5910(86)80110-3.
[42] P. Basu, L. Cheng, An analysis of loop seal operations in a circulating fluidized bed, Chem. Eng. Res. Des. 78 (2000) 991–998, https://doi.org/10.1205/026387600528102.
[43] S.W. Kim, S.D. Kim, D.H. Lee, Pressure balance model for circulating fluidized beds with a loop-seal, Ind. Eng. Chem. Res. 41 (2002) 4949–4956, https://doi.org/10.1021/ie0202571.
[44] Z. Tang, P. Gao, Y. Sun, Y. Han, Experimental study on fluidization characteristics of different-sized particles in a U-type reduction chamber, Adv. Powder Technol. 30 (2019) 2430–2439, https://doi.org/10.1016/j.apt.2019.07.028.
[45] A. Chinsuwan, A mathematical model for predicting the flow behavior through a CFB reactor U type loop - seal, Int. J. Heat Mass Transf. 177 (2021), https://doi.org/10.1016/j.ijheatmasstransfer.2021.121541.
[46] Q. Wang, H. Yang, P. Wang, J. Lu, Q. Liu, H. Zhang, L. Wei, M. Zhang, Application of CPFD method in the simulation of a circulating fluidized bed with a loop seal Part I-Determination of modeling parameters, Powder Technol. 253 (2014) 814–821, https://doi.org/10.1016/j.powtec.2013.11.041.
[47] Q. Wang, H. Yang, P. Wang, J. Lu, Q. Liu, H. Zhang, L. Wei, M. Zhang, Application of CPFD method in the simulation of a circulating fluidized bed with a loop seal Part II-Investigation of solids circulation, Powder Technol. 253 (2014) 822–828, https://doi.org/10.1016/j.powtec.2013.11.040.